Journal of Polymer Research (2022) 29: 384
https://doi.org/10.1007/s10965-022-03237-6

ORIGINAL PAPER

Preparation and properties of hemoglobin (Hb)-imprinted poly (ionic liquid)s via seATRP in only 5 µL Volumes

Ailu Cui[1] · Zuan Yang[1] · Xuewei Feng[1] · Huanying Zhao[1] · Peiran Meng[1] · Yanxuan Xie[1] · Linan Miao[1] · Yue Sun[1]

Received: 9 April 2022 / Accepted: 10 August 2022 / Published online: 15 August 2022

Abstract

Hemoglobin (Hb) imprinted poly (ionic liquid)s (HIPILs) were fabricated on the surface of Pt wire modified with nano-gold (nAu) via simplified electrochemically mediated atom transfer radical polymerization (seATRP) in only 5 µL volumes. The micro upgrade seATRP was mainly carried out by two platinum wires electrode. The one platinum wire was bare and applied as the counter electrode, the other one was modified segmentally, which made it could be used both as a catalytic electrode of seATRP and the substrate of HIPILs. The HIPILs were prepared by using Hb as the template, 1-vinyl-3-propyl-imidazole sulfonate (VPIS) ionic liquids and N, N′-methylene bis-acrylamide (MBA) as the functional monomer and cross-linking agent of HIPILs, respectively. When a constant current was applied to the catalytic electrode, Fe (III) in Hb would be reduced to Fe (II), seATRP of VPIS would be triggered on the surface of Pt/nAu electrode. After Hb was removed, the HIPILs modified electrode (Pt/nAu/HIPILs) was obtained. The Pt/nAu/HIPILs electrode was characterized by scanning electron microscopy (SEM), X-ray photoelectron spectroscopy (XPS), cyclic voltammetry (CV), and electrochemical impedance spectroscopy (EIS). Further experiments indicated that the Pt/nAu/HIPILs electrode could be utilized as electrochemical sensor to determine Hb by differential pulse voltammetry (DPV). The linear response range was $1.0\times10^{-12}\sim1.0\times10^{-1}$ mg/mL and the detection limit was 3.29×10^{-13} mg/mL ($S/N=3$). Compared with other Hb sensors based on imprinting polymers, the broader linear range and lower detection limit suggested the promising prospect of the biosensor.

Keywords Imprinted poly (ionic liquid)s · seATRP · 5 µL · Biosensor

Introduction

Molecularly imprinted polymers (MIPs) are recognition materials prepared by a template-assisted synthesis [1]. On account of its unique advantages such as physicochemical and biochemical resistance, low cost, high affinity, and good stability [2–5], MIPs have been widely exploited in diverse applications, such as drug delivery, cosmetics, virus determination, and chemical sensing [6–9]. Polymerization method is significant for the preparation of MIPs. Atom transfer radical polymerization (ATRP) has become one of the most extensively used techniques to emerge MIPs owing to its narrow molecular weight distributions, pre-determined molecular weights, as well as control polymer topology [10–12]. ATRP can be triumphantly utilized in various technologies. In recent years, extensive publicity has been paid to electrochemically mediated ATRP (eATRP) due to versatility in synthesis, construction of functional surfaces, and low catalyst concentration [13–15]. eATRP is ordinarily implemented in three electrode systems, which includes a working electrode (WE), a counter electrode (CE), and a reference electrode (RE) with either potentiostatic or galvanostatic process [16]. The setup usually requests sufficient large volumes (> 10 mL) to ensure appropriate stirring and contact of all electrodes with the polymerization solution [17].

Polymerization volume from mL to µL levels has a series of advantages. Above all, small volume adheres to 'Green Analytical Chemistry' standards and the principles of sustainable development [18]. Moreover, it has positive effect on environmental aspects including preventing/minimizing chemical waste and generating less contamination. Afterward, it is more conducive to address budget-related needs to employ precious or high-performance materials. To wind up with, it not only assures conscientiously utilizing chemical resources, but also implements easily high-throughput,

✉ Yue Sun
yuesun@lnnu.edu.cn

[1] School of Chemistry and Chemical Engineering, Liaoning Normal University, Dalian 116029, China

flash-synthesis [19]. However, small-volume polymerization is not easy to come true at this stage. Besides requiring sufficient large volumes (> 10 mL) to assure that all electrodes are in full contact with the polymerization solution, small-volume polymerization aggravates the challenge of deoxygenation of polymerization solution. In General, radical polymerizations are operated in anaerobic environments because molecular oxygen is a valid radical quencher [20]. The commonly used methods include flushing with inert atmospheres (*e.g.* argon, nitrogen), thiol-ene reactions under ultraviolet irradiation, utilizing potato fruit juice (PFJ) bioplastic films, reacting in a glovebox, and freeze – pump – thaw technology [21–25]. Although these methods have been successfully applied in the preparation of polymers, they have obvious drawbacks of time consuming, intensive labor procedures, and loss of polymerization volume [26–28]. Therefore, it is still a big challenge to achieve polymerization from mL down to μL levels for eATRP.

A simplified electrochemically mediated ATRP (seATRP) was the improved eATRP developed in recent years. SeATRP has been applied to prepare polymers owing to its superior controllability in the absence of traditional ligand, the minimization of the ohmic drop, and good control of reaction kinetics [29–31]. For example, Chmielarz et al. prepared poly(ethylene oxide)-block-poly(butyl acrylate) copolymers via seATRP utilizing only 1 ppm of Cu^{II} complex. It was the limit of a successful well-controlled polymerization [32]. Zaborniak et al. synthesized star and comb polymers with long poly(n-butyl acrylate) side chains by seATRP using ca. 100 ppm of copper catalyst. The polymers had low dispersity and narrow molecular weight distributions [33]. Chmielarz et al. prepared β-cyclodextrin-poly(n-butyl acrylate) (β-CD-PBA) star-shaped amphiphilic polymers via seATRP procedure utilizing only 50 ppm Cu^{II} complex. The β-CD-PBA star polymers had the living nature prepared by seATRP [34]. As reported, seATRP did not implore the separation of cathodic and anodic compartments in the polymerization system, and could simplify the reaction system by sacrificing counter electrode [35]. Therefore, it is very attracting and promising to decrease the polymerization volume from mL to μL. However, to date, there have been no reports on micro-upgrading of seATRP, nor on the application of seATRP to MIPs preparation.

Ionic liquids (ILs) are salts with melting points at or below 100 ℃, which comprise organic cations and organic/inorganic anions [36]. They possess unique physicochemical properties including high thermal stability, tunable viscosity, and solvation capabilities [37]. ILs have been reported in recent years. It is applied in the synthesis of MIPs as functional monomers. For example, Xie et al. synthesized a novel molecularly imprinted fluorescent sensor with 3-[(7-methoxy-2-oxo-2*H*-chromen-4-yl) methyl]-1-vinyl-1*H*-imidazol-3-ium bromide as the functional monomer. The fluorescent sensor had short detection time (0.5 min), high fluorescence intensity, good selectivity, and excellent sensitivity (limit of detection = 0.8 nM) for 4-NA [38]. Lu et al. reported a novel electrochemical sensor for rutin determination based on molecularly imprinted poly (ionic liquid) with 1-allyl-3-ethyl imidazolium bromide as the functional monomer. The sensor had good linearity from 0.03 to 1 μM, and the limit of detection was generated as 0.01 μM (*S/N* = *3*) [39]. Wu et al. designed molecularly imprinted electrochemical sensor for alpha-fetoprotein (AFP) using 1-[3-(N-cystamine) propyl]-3-vinylimidazolium tetrafluoroborate ionic liquid as the functional monomer. The sensor showed a good linear response to AFP in the concentration range of 0.03 ng/mL ~ 5 ng/mL. The detection limit was estimated to be 2 pg/mL [40].

Considering the advantages of ionic liquids, small-volume polymerization, and seATRP, in this paper, hemoglobin (Hb) imprinted poly (ionic liquid)s (HIPILs) were prepared via Hb catalyzed seATRP on the surface of Pt wire modified with nano-gold (nAu) in only 5 μL polymerization volumes. As shown in Fig. 1, two platinum wires electrode were utilized to achieve small-volume seATRP. The one bare platinum wire electrode was applied as the counter electrode, the other was used as the working electrode. The working electrode had a critical end of 2 mm. One mm was used as a catalytic electrode of seATRP, which was modified with nano-gold (nAu), poly toluidine blue (PTB) and nano-Pt (nPt). The other one mm was exploited as the substrate of HIPILs, which was embellished with nano-gold and initiator of seATRP. Hb was used as both the template of imprinting polymers and the catalyst of seATRP. 1-vinyl-3-propyl-imidazole sulfonate (VPIS) ionic liquids and N, N′-methylene bis-acrylamide (MBA) were selected as the functional monomer and cross-linking agent, respectively. When a constant current was applied to the catalytic electrode of seATRP, Fe (III) in Hb would be reduced to Fe (II), then the polymerization of VPIS would be triggered [41]. After Hb was removed, the HIPILs modified electrode (Pt/nAu/HIPILs) was obtained. The Pt/nAu/HIPILs electrode was characterized by scanning electron microscopy (SEM), X-ray photoelectron spectroscopy (XPS), cyclic voltammetry (CV), and electrochemical impedance spectroscopy (EIS). Further experiments indicated that the Pt/nAu/HIPILs electrode could be utilized as electrochemical sensor to determine Hb by differential pulse voltammetry (DPV).

Materials and methods

Chemicals

Pt wire (Φ = 0.5 mm) was from Chenhua Instruments Co. (Shanghai, China). VPIS ionic liquids were purchased from Shanghai Cheng Jie Chemical Co. Ltd. (Shanghai,

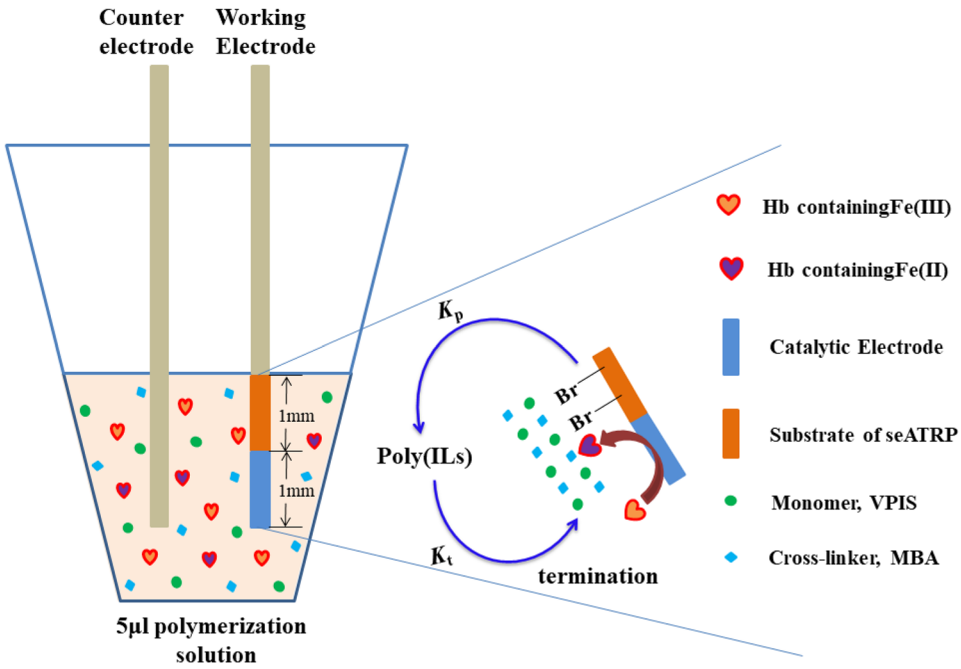

Fig. 1 Preparation scheme of Pt/nAu/HIPILs electrode via Hb catalyzed seATRP

China). MBA, sodium dodecyl sulfate (SDS), potassium ferricyanide, potassium ferrocyanide, potassium dihydrogen phosphate, disodium hydrogen phosphate, glacial acetic acid, sodium acetate, and anhydrous ethanol were obtained from Kemiou Chemical Co. (Tianjin, China). Chloroauric acid ($HAuCl_4{\cdot}4H_2O$) and chloroplatinic acid ($HPtCl_6{\cdot}6H_2O$) were provided by Beijing Chemical Plant (Beijing, China). Pepsinogen (PG, MW 35 kDa), superoxide dismutase (SOD, MW 34 kDa), laccase (Lac, MW 66 kDa), lysozyme (Lyz, MW 14.4 kDa), and hemoglobin (Hb, MW 65 kDa) were supplied by Solarbio Inc (Beijing, China). Toluidine blue (TB) was obtained from Yuanye biological Inc (Shanghai, China). Phosphate buffered solution (PBS, pH 7.0) was prepared by using 0.02 mol/L Na_2HPO_4 and 0.02 mol/L KH_2PO_4. Acetate buffer solution (ABS, pH 5.0) was prepared by 0.01 mol/L CH_3COOH and 0.01 mol/L CH_3COONa. All chemicals were of analytical reagent grade. All the water used in the experiments was the hyperpure water (resistivity > 18 MΩ • cm).

Apparatus

CV, EIS, seATRP, and DPV were executed with a CHI660D electrochemical workstation (Chenhua, Shanghai, China). CV characterization was performed in PBS (pH 7.0) containing 0.1 mol/L^{-1} KCl + 5 mmol/L $[Fe(CN)_6]^{3-/4-}$ at a scanning rate of 100 mV s^{-1}. The potential was set between -0.2 V and 0.6 V. The sampling interval, the polarization time, and the sensitivity were set as 0.001 V, 2 s, and 10^{-4} A/V, respectively.

EIS was conducted in the same solution to the CV characterization within the frequency range of 0.05 Hz to 10 kHz.

Surface topographic characteristics of the modified electrode was acquired by SEM (SU8010, Hitachi, Japan).

XPS was used to study the chemical composition of the modified electrode, which was obtained with Thermo ESCALAB 250Xi spectrometer using a monochromatic Al Kα radiation.

Preparation of Hb-imprinted PILs via seATRP in only 5 μL Volumes

Hb-imprinted PILs were prepared in five steps, which was shown in Fig. 2. (1) Nano-gold was fabricated on the clean platinum wire surface by electrodeposition. The clean platinum wire was used as working electrode, and the SCE and another platinum wire were used as reference electrode and counter electrode, respectively. Three electrodes were placed in 1% (w/v) $HAuCl_4$ solution (prepared in 0.1 mol/L pH 5.0 ABS). Among these, the depth of the working electrode in the solution was controlled to be 2 mm. After the chronoamperometry experiment at—0.9 V for 400 s, nano-gold was electrodeposited on the Pt electrode and Pt/nAu electrode was obtained. (2) According to the literature [42], the Pt/nAu electrode was inserted in thiol bromide initiator solution overnight, the depth of the electrode in the solution was controlled to be 2 mm. The thiol bromide initiator (4-mercaptophenyl-2-bromo-2-methylpropanoate, 4-HTP-Br) would decorate

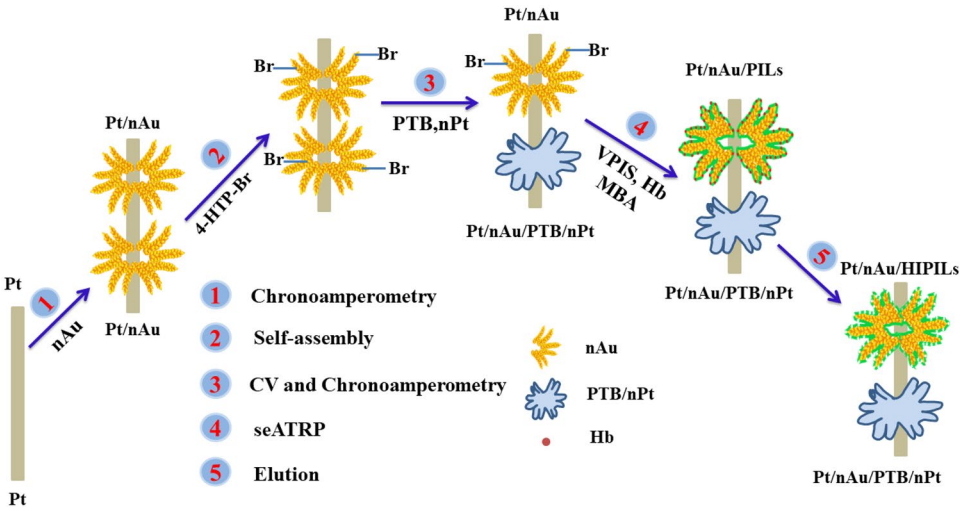

Fig. 2 Preparation scheme of Pt/nAu/HIPILs

on the surface of Pt/nAu electrode. (3) Poly toluidine blue (PTB) and nano-Pt were synthesized on the surface of Pt/nAu electrode. The Pt/nAu electrode was used as working electrode and the depth of it in the solution was controlled to be 1 mm. The SCE and clean platinum wire were used as reference electrode and counter electrode, respectively. The CV was run from -0.8 to 1.3 V in 5×10^{-5} mol/L TB (prepared in 0.1 mol/L pH 5.0 ABS) with a scan rate of 0.05 V/s. After rinsing with PBS five times, Pt/nAu/PTB was obtained. Nano-Pt was electrodeposited on Pt/nAu/PTB by chronoamperometry at -0.7 V (vs. SCE) for 100 s in 0.01 mol/L $HPtCl_6$ solution (prepared in 0.1 mol/L pH 5.0 ABS). (4) Poly (ionic liquid)s were polymerized on the surface of Pt/nAu electrode. As shown in Fig. 2, the electrode mentioned above was inserted in the polymerization solution of only 5 µL volumes and the depth of it in the solution was controlled to be 2 mm. This electrode would be used both as the catalytic electrode of seATRP and the substrate of polymerization. Another platinum wire was used as counter electrode. The polymerization solution contained VPIS (0.1 mol/L, functional monomer), MBA (0.1 mol/L, crosslinking agent), Hb (2 mg/ml), and PBS (pH 7.0) as solvent. When a constant current of 1 mA was applied to Pt/nAu/PTB/nPt by chronoamperometry at 0.46 V (vs. SCE). The run time and the sensitivity were set as 3600 s and 10^{-3} A/V, respectively. Fe (III) in Hb would be reduced to Fe (II) (catalyst for ATRP) on the electrode surface and trigger the polymerization of ILs [43]. Except the applied current, other parameters included a sample interval of 0.1 s and a sensitivity of 1×10^{-4} A/V. (5) The Hb was removed from the electrode by soaking in 10% (v/v) CH_3COOH solution containing 10 g/L SDS for 1 h. After washing with PBS three times, the Hb-imprinted PILs (Pt/nAu/HIPILs) were prepared on the surface of the electrode.

Preparation of non-imprinted PILs electrode

For comparison with Hb-imprinted PILs electrode, a non-imprinted PILs electrode was prepared by the traditional free radical polymerization method in the absence of Hb. Ammoniumpersulfate (0.9 mol/L) was used as initiator to polymerize VPIS (0.1 mol/L, functional monomer), and MBA (0.1 mol/L, crosslinking agent) at room temperature for 5 h on the surface of Pt/nAu electrode. The obtained Pt/nAu/NIPILs electrode was stored under a N_2 atmosphere before use.

Determination of Hb

The determination of Hb by Pt/nAu/HIPILs electrode was studied by the DPV method. Before test, the Pt/nAu/HIPILs electrode was incubated in different concentrations of Hb solution for 5 min at room temperature and rinsed three times with PBS. The DPV was operated from -0.2 to 0.6 V in PBS containing 5 mmol/L $[Fe(CN)_6]^{3-/4-}$, against the SCE reference electrode. An increment potential of 4 mV, polarization time of 2 s, amplitude of 50 mV, a sensitivity of 1×10^{-4}A/V, a pulse width of 0.2 s, sampling interval of 0.0167 s, and a pulse period of 0.5 s were set as the corresponding DPV parameters. Quantitative analysis of Hb was conducted as the signal response (ΔI), which was the reduction of the peak current in the presence and absence of Hb.

Results and discussion

Characterization of Pt/nAu/HIPILs

The morphologies of the modified electrodes were observed by SEM. As displayed in Fig. 3A, the bare Pt wire electrode showed a plane structure. When it was modified with

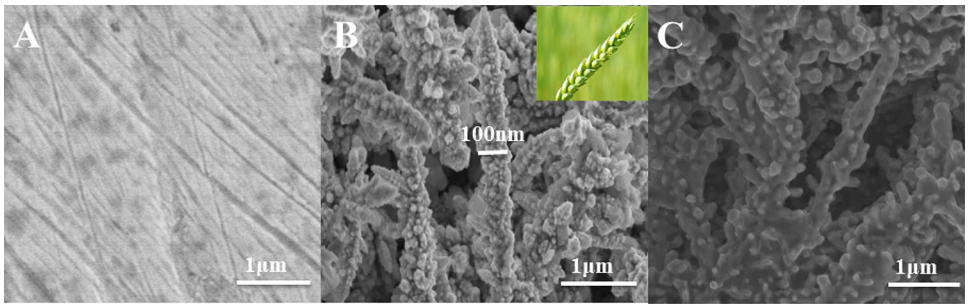

Fig. 3 The SEM images of bare Pt wire (**A**), Pt/nAu (**B**) and Pt/nAu/PILs (**C**). The inset was the picture of wheat ear

nano-gold (Pt/nAu electrode, in Fig. 3B), the surface of electrode exhibited branchlike structure that looked like wheat ear (shown in the inert). As could be seen, the mean diameter of 'wheat ear' was about 100 nm. Furthermore, CV was used to investigate the effect of nano-gold on the surface area of the electrode [44], the oxidation peak current in the obtained CV curve was plotted against the square root of sweep velocity, as described in Fig. SA and SB. According to the Randles–Sevcik equation [45], the area of the Pt/nAu electrode was about twice that of the Pt electrode (Fig. SC). After the polymerization of ILs on the surface of Pt/nAu (Pt/nAu/PILs electrode, in Fig. 3C), the small grain structure of the 'wheat ear' was covered by the polymer, leaving only a few large protrusions. From the results of Fig. 3, the area of the electrode was increased greatly by nano-gold and seATRP of only 5 μL polymerization volumes was successfully conducted.

The surface chemical composition of Pt/nAu/PILs electrode before and after removing of Hb was characterized by XPS, and the results were elucidated in Fig. 4. As shown in Fig. 4A, the binding energy of elements were observed at 531.40 eV, 399.90 eV, 287.25 eV, 83.85 eV, and 70.75 eV, respectively. On account of previous literature reported, they were identified as the characteristic peaks of O 1 s, N 1 s, C 1 s, Au 4f, and Br 3d, respectively [46, 47]. The exposure of reactive Br 3d to the surface demonstrated that seATRP was implemented [48]. The binding energy at 713.20 eV in the inset of Fig. 4A was the fine XPS of Fe 2p [49]; because Fe was only originated from Hb, thus indicating the existence of Hb in Pt/nAu/PILs and the polymerization was catalyzed by Hb. After removing of Hb, the XPS spectrum of obtained Pt/nAu/HIPILs was also estimated by XPS. The result was displayed in Fig. 4B. The peaks of O 1 s, N 1 s, C 1 s, Au 4f, and Br 3d exhibited the binding energy at the similar position compared with Pt/nAu/PILs. The disappearance of Fe 2p binding energy proved that Hb had been removed from the polymers and Pt/nAu/HIPILs was successfully prepared.

CV and EIS were used to characterize the electrochemical behavior of the electrode after each modification step. Figure 5A was the CV of different modified electrodes in PBS (pH 7.0) solution containing 0.1 mol·L^{-1} KCl + 5 mmol L^{-1} $[Fe(CN)_6]^{3-/4-}$. As expected, there

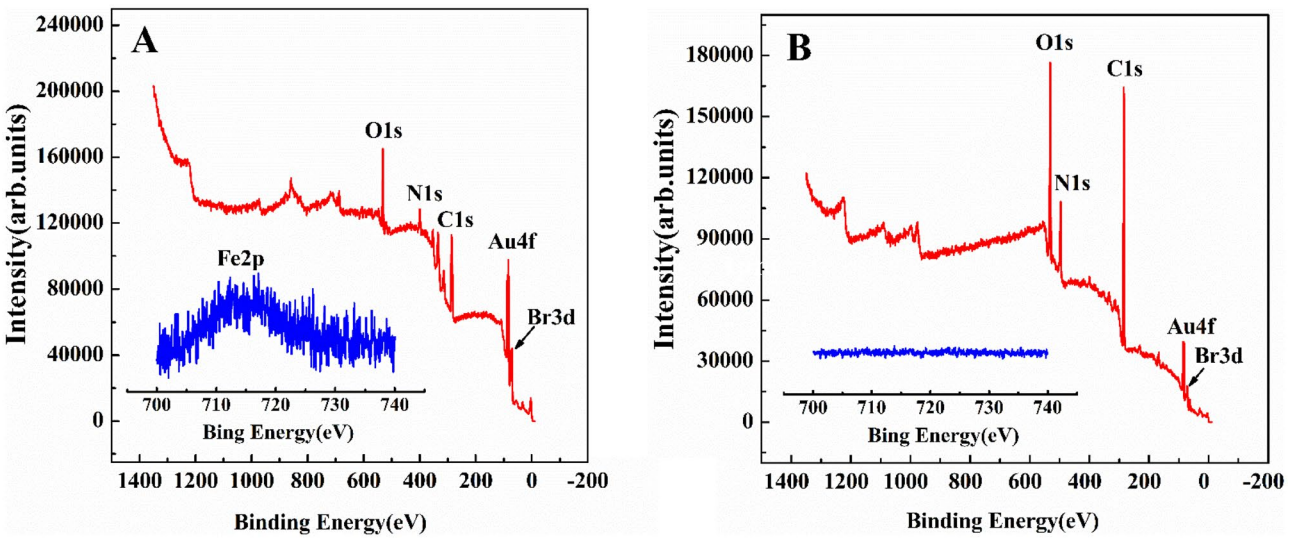

Fig. 4 The XPS of Pt/nAu/PILs before (**A**) and after (**B**) removing of Hb

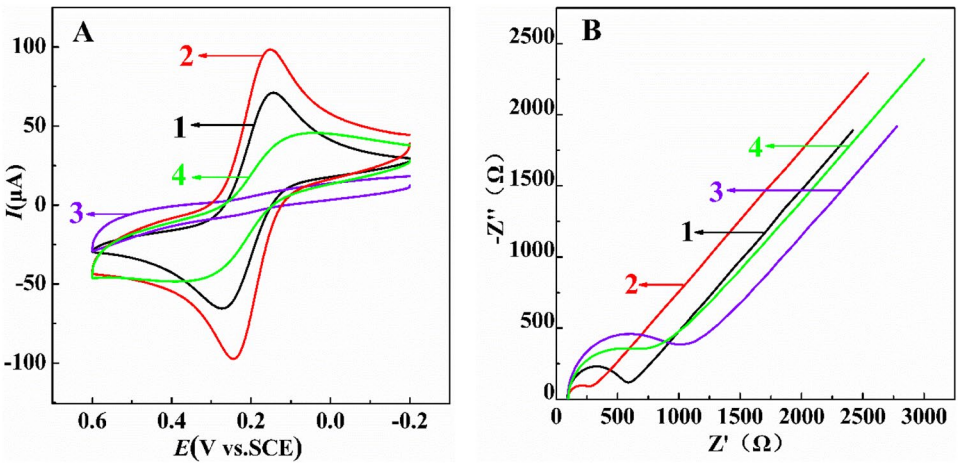

Fig. 5 The CV (**A**) and EIS (**B**) characterization of the stepwise modified electrodes (1-bare Pt wire, 2- Pt/nAu, 3-Pt/nAu/PILs, 4-Pt/nAu/HIPILs) in PBS (pH 7.0) containing 5 mmol/L $[Fe(CN)_6]^{3-/4-}$ and 0.1 mol/L KCl. The scanning rate of CV was 100 mV/s

was an approximately quasi-reversible redox peak of $[Fe(CN)_6]^{3-/4-}$ probe at the bare Pt wire (Fig. 5A curve 1), showing the conducting nature of bare Pt wire electrode [50]. When the bare Pt wire was modified by nano-gold (Pt/nAu) (Fig. 5A curve 2), its peak current increased significantly indicating that nanomaterials enlarged the effective electrode surface area and improved electron transfer rate [51]. For Pt/nAu/PILs electrode (Fig. 5A curve 3), the peak current decreased sharply. The reason for this phenomenon might be that the poly (ILs) formed on the surface of electrode, which acted as an inert material and hindered the diffusion of $[Fe(CN)_6]^{3-/4-}$ to electrode. After removing the Hb molecule, the peak current of the electrode (Pt/nAu/HIPILs) was obviously elevated (Fig. 5A curve 4). This might be because the stripping of Hb, which formed the imprinted holes on the surface of the electrode, leading the $[Fe(CN)_6]^{3-/4-}$ probe easier diffusion and showing the higher peak current of CV.

EIS was the most common techniques used for probing the features of a surface modified electrode. Figure 5B showed the EIS of stepwise modified electrodes. The bare Pt wire electrode showed a relatively high R_{ct} (Fig. 5B curve 1). After being modified with nano-gold, the EIS revealed a decrease of R_{ct} of the redox probe on the resulting electrode (Fig. 5B, curve 2). It was evident that introduction of nano-gold improved the conductivity and enlarged surface area of the electrode [52]. By formation of poly (ILs) on the Pt/nAu surface (Fig. 5B curve 3), an obvious increase of R_{ct} was obtained. This might be attributed to the inertness of polymers. After removing Hb (Fig. 5B curve 4), R_{ct} became smaller than that of Pt/nAu/PILs, indicating that the imprinted holes appeared on Pt/nAu/HIPILs, driving the proximity of $[Fe(CN)_6]^{3-/4-}$ probe. Compositing the results of SEM, XPS, CV, and EIS, seATRP of only 5 μL volumes could be implemented and HIPILs had been successfully prepared on the surface of electrode.

Optimization of experimental parameters

The typical conditions including polymerization time and polymerization currents, which were vital parameters in the experiment and had an influence on the sensing

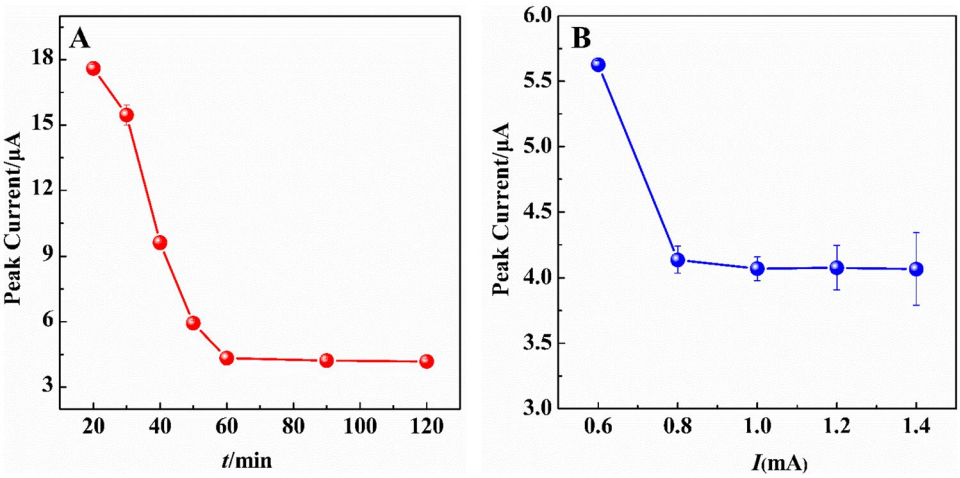

Fig. 6 The condition selection of time (**A**) and current (**B**)

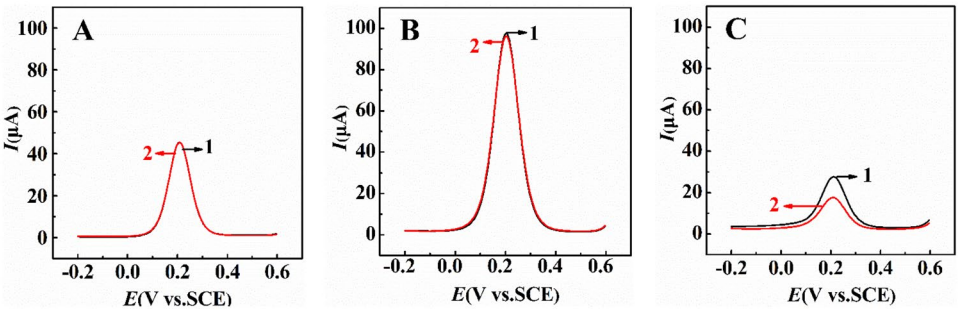

Fig. 7 The DPV signal response of different modified electrodes: **A** bare Pt wire; **B** Pt/nAu; **C** Pt/nAu/HIPILs:1-before combining with Hb solution, 2-after combining with Hb solution (10^{-12} mg/mL)

performance of Pt/nAu/PILs biosensor, were investigated by DPV method. $[Fe(CN)_6]^{3-/4-}$ was used as the probe of DPV to indicate the electron transfer ability of PILs. As could be seen in Fig. 6A, with the increasing of polymerization time from 20 to 60 min, the peak current dropped extremely indicating that the polymer layer became thicker and thicker, which prevented the $[Fe(CN)_6]^{3-/4-}$ from reaching the electrode surface. When the polymerization time further increased from 60 min, there was nearly no change in the peak current. Therefore, polymerization time of 60 min (1 h) was selected as subsequent experiments. Figure 6B showed the effect of polymerization currents on the Pt/nAu/PILs. As could be seen, increasing the polymerization currents from 0.6 to 1 mA, the DPV peak current of Pt/nAu/PILs electrode decreased gradually. It might be increasing peak current increased the polymerization efficiency, thickened the polymer layer, and hence increased the difficulty of probe ions reaching the electrode surface. However, when the polymerization current increased from 1.0 to 1.4 mA, the DPV peak current of Pt/nAu/PILs electrode had no evident change. From the results of Fig. 6B, the current of seATRP was optimal to be 1.0 mA.

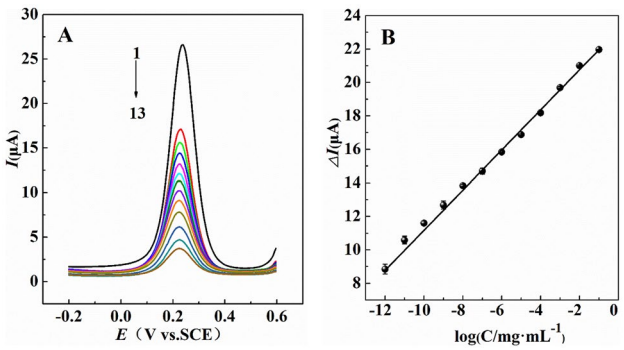

Fig. 8 **A** The DPV curves of Pt/nAu/HIPILs in PBS containing 0.1 mol·L^{-1} KCl + 5 mmol·L^{-1} $[Fe(CN)_6]^{3-/4-}$after rebinding with Hb (concentrations of Hb from curve 1 to curve 13 were 0, 10^{-12}, 10^{-11}, 10^{-10}, 10^{-9}, 10^{-8}, 10^{-7}, 10^{-6}, 10^{-5}, 10^{-4}, 10^{-3}, 10^{-2}, 10^{-1} mg/mL). **B** The calibration plot of Pt/nAu/HIPILs

Electrochemical response to Hb for the different electrodes

The electrochemical response of bare Pt wire, Pt/nAu, and Pt/nAu/HIPILs were compared by DPV and shown in Fig. 7. It could be seen that the bare Pt wire electrode had almost the same DPV curve before (Fig. 7A, curve 1) or after (Fig. 7A, curve 2) combining with Hb solution (10^{-12} mg/mL), which indicated that bare Pt wire electrode had no electrochemical response toward Hb. The similar phenomenon could be observed on Pt/nAu electrode (Fig. 7B). It was worth mentioning that the DPV peak current of Pt/nAu were higher than that of Pt wire due to the large surface area and good electron transfer capability of nano-gold, which was consistent with the results of CV and EIS (Fig. 5). As shown in Fig. 7C, the DPV peak current of Pt/nAu/HIPILs after combining with Hb (Fig. 7C, curve 2) decreased significantly comparing with that of before combining (Fig. 7C, curve 1), indicating that the Pt/nAu/HIPILs had good electrochemical response to Hb.

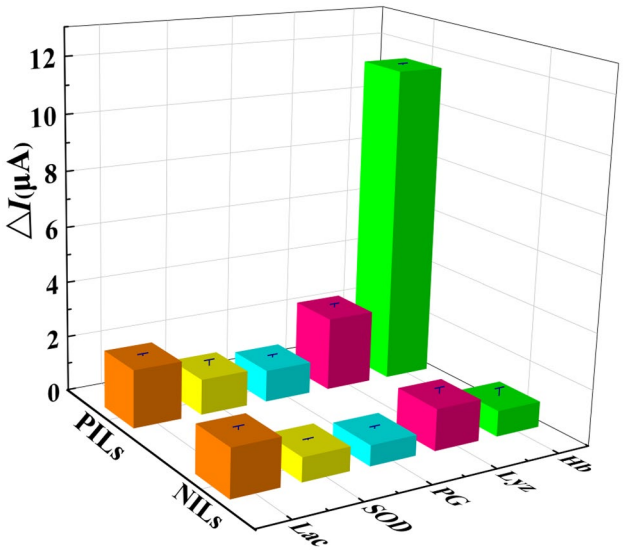

Fig. 9 Signal responses of Pt/nAu/HIPILs (PILs) and Pt/nAu/NIPILs (NILs) for the template (Hb) and interferents (Lyz, PG, SOD, Lac)

Table 1 Comparison of the linear response range of Pt/nAu/HIPILs and other materials for the determination of Hb[a]

Materials	Detection method	Linear range (mg/mL)	Detection limit (mg / ml)	References
Carbon quantum dots fluorescent probes derived from cholesterol	Fluorescence	6.4×10^{-3} ~ 1.8×10^{-1} 6.4×10^{-5}	1.53×10^{-3} 8.32×10^{-6}	[54]
Persistent label free probe based on luminescence	Continuous luminescence	6.4×10^{-5} ~ 3.2×10^{-3}	8.32×10^{-6}	[55]
Multi-walled carbon nanotubes@Fe_3O_4@SiO_2	Chemiluminescence	5.0×10^{-10} ~ 7.0×10^{-7}	1.5×10^{-10}	[56]
Carbon paste electrode ionic liquid	DPV	6.4×10^{-7} ~ 6.4×10^{-1}	3.3×10^{-7}	[57]
Protein molecularly imprinted polymer	DPV	1.0×10^{-12} ~ 1.0×10^{-1}	3.29×10^{-13}	This work

For facilitate comparison, the data units were converted

Determination of Hb by DPV

The Pt/nAu/HIPILs electrode was used as an electrochemical biosensor to detect Hb by DPV. Figure 8 demonstrated the DPV curves of the Pt/nAu/HIPILs after rebinding with a series of concentrations of Hb solutions. As could be seen from Fig. 8A, with the increasing of Hb concentration, the DPV peak current of the Pt/nAu/HIPILs decreased gradually. This might be owing to the combination of Hb and imprinted cavity, $[Fe(CN)_6]^{3-/4-}$ was blocked from reaching the surface of the electrode [53]. According to the relation of DPV current difference (signal response, ΔI) with Hb concentration, the linear range of detecting Hb by Pt/nAu/HIPILs was from 1.0×10^{-12} to 1.0×10^{-1} mg/ml. As shown in Fig. 8B, the linear regression equation was ΔI (μA) = 1.162 log C (mg/ml) + 23.036 with a correlation coefficient of 0.996. The detection limit (LOD, $S/N = 3$) of 3.29×10^{-13} mg/mL could be estimated.

In order to highlight the superiority of the biosensor, the analytical performance of the Pt/nAu/HIPILs was compared with other sensors for Hb detection including fluorescence, chemiluminescence, continuous luminescence, and electrochemical method. It could be clearly seen from Table 1 that the prepared Pt/nAu/HIPILs electrode possessed wider detection range and lower detection limit.

Selectivity of Pt/nAu/HIPILs electrode

The selectivity of Pt/nAu/HIPILs electrode toward Hb was evaluated by using different protein including pepsin (PG, MW, 35 kDa), superoxide dismutase (SOD, MW, 34 kDa), laccase (Lac, MW, 66 kDa), and lysozyme (Lyz, MW, 14.4 kDa) as interferents. The signal responses (ΔI) of Pt/nAu/HIPILs and Pt/nAu/NIPILs toward each protein (10^{-10} mg/ml) were determined by DPV. As could be seen from Fig. 9, the response signal(ΔI) of the Pt/nAu/HIPILs electrode to Hb was 11.42μA, which was 9.96, 8.92, 5.7, and 4.32 times of PG, SOD, Lac, and Lyz, respectively. The results showed that the Pt/nAu/HIPILs electrode could be used as an electrochemical sensor and had better selectivity toward Hb. The selectivity of the electrode was also further evaluated by the imprinting factor (IF), which was calculated as following: $IF = \Delta I_{(PILs)}/\Delta I_{(NILs)}$ [46]. The IF values of Hb, SOD, Lyz, PG, and Lac were 12.32, 1.49, 1.5, 1.57, and 1.77, respectively. The maximum IF value of Hb indicated that the Pt/nAu/HIPILs electrode had better recognition performance for Hb.

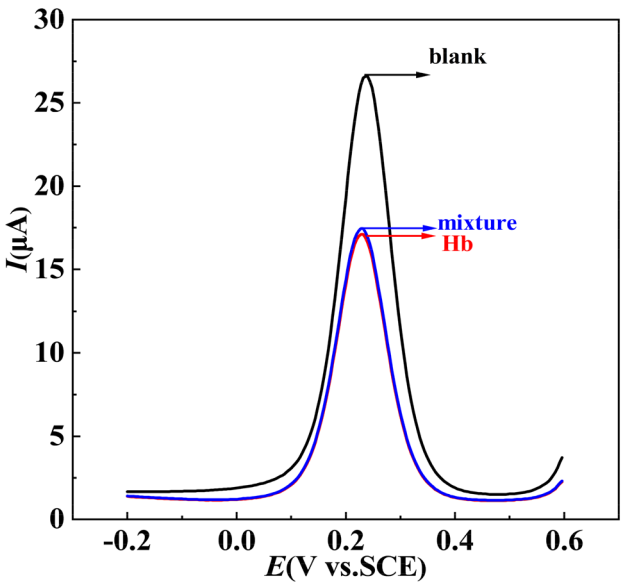

Fig. 10 DPV curves of imprinted polymer modified electrode: mixed solution and Hb solution detection by Pt/nAu/HIPILs

Table 2 Detection of Hb in real samples (n = 3)

Analyze	Original sample concentration* (mg/mL)	Added (mg/mL)	Detection concentration (mg/mL)	Recovery(%)	RSD (%)
Hb	1.0×10^{-4}	1.00×10^{-4}	2.08×10^{-4}	108.9	1.97
		2.00×10^{-4}	3.45×10^{-4}	105.4	3.31
		5.00×10^{-4}	5.98×10^{-4}	98.4	2.18

*The concentration detected by blood cell analyzer

Repeatability, reproducibility, and competition of Pt/nAu/HIPILs electrode

In order to determine the repeatability of the Pt/nAu/HIPILs sensor, 10^{-12} mg/mL Hb (in PBS) was analyzed five times by the same Pt/nAu/HIPILs electrode repeatedly at the same day. The relative standard deviation (RSD) was 1.01%, implying that the Pt/nAu/HIPILs sensor had good consistency and could be reused. In addition, to evaluate the reproducibility of the Pt/nAu/HIPILs sensor, five Pt/nAu/HIPILs electrodes were incubated in the same concentration (10^{-12} mg/ml) of Hb solution for 5 min, washed with PBS for three times, and then tested for DPV. The DPV was operated from -0.2 to 0.6 V in PBS containing 5 mmol/L $[Fe(CN)_6]^{3-/4-}$, against the SCE reference electrode. An increment potential of 4 mV, polarization time of 2 s, amplitude of 50 mV, a sensitivity of 1×10^{-4}A/V, a pulse width of 0.2 s, sampling interval of 0.0167 s, and a pulse period of 0.5 s were set as the corresponding DPV parameters. The DPV was conducted before or after incubating, and the obtained signal responses (ΔI) was recorded. The RSD was 2.78%, indicating that the Pt/nAu/HIPILs sensor possessed good reproducibility.

The competition of Pt/nAu/HIPILs electrode was carried out between mixed solution (containing Hb, Lyz, PG, SOD, Lac) and Hb solution by DPV. The results were shown in Fig. 10. The response signal(ΔI) of the Pt/nAu/HIPILs electrode toward Hb solution was 9.092μA, which was 0.916 times that of mixed solution. The results showed that the Pt/nAu/HIPILs electrode had good selectivity for Hb in the presence of competitors.

Application of Pt/nAu/HIPILs electrode

To investigate the reliability of the Pt/nAu/HIPILs electrode, the actual sample of bovine blood was further detected by standard addition method. The bovine blood sample was processed according to the literatures [58] and analyzed by hematology analyzer. 10, 20, and 50 μL Hb standard solution with concentration of 10^{-1} mg/mL were added into the bovine blood sample of 10 mL, respectively. According to the linear equation ΔI (μA) = 1.162 logC (mg/mL) + 23.036, the detection concentration, spiked recovery rate, and RSD could be calculated, and the results were shown in Table 2. It could be seen that the recovery of Pt/nAu/HIPILs for bovine blood sample was from 98 to 109% and the RSD was less than 4%, implying that the Pt/nAu/HIPILs sensor could be used for the analysis of actual samples.

Conclusions

In conclusion, a novel electrochemical imprinted biosensor (Pt/nAu/HIPILs) was conducted by seATRP in only 5 μL volumes. The HIPILs were prepared by using Hb as the template, VPIS ionic liquids and MBA as the functional monomer and cross-linking agent, respectively. Firstly, the polymerization time and current were selected to be 1 h and1.0 mA. Secondly, the biosensor was examined by SEM, XPS, CV, and EIS. Finally, the Pt/nAu/HIPILs electrode was used as a biosensor and successfully applied for the detection of Hb by DPV. The Pt/nAu/HIPILs electrode showed that the linear range was $1.0\times10^{-12}\sim1.0\times10^{-1}$ mg/ml, and the detection limit was 3.29×10^{-13} mg/ml ($S/N = 3$). The Pt/nAu/HIPILs electrode also illustrated good selectivity in the presence of Lyz, PG, SOD, and Lac. In a word, the work of this paper reported a worthwhile way for the preparation and application of biosensor based on small-volume polymerization via seATRP.

Supplementary Information The online version contains supplementary material available at https://doi.org/10.1007/s10965-022-03237-6.

Acknowledgements This work was supported by Nature Science Foundation of Liaoning Province (No. 2021-MS-273), Liaoning BaiQianWan Talents Program (No. 2020921109), High-end Research Incubation Scheme of Liaoning Normal University (No. GD20L001), and Undergraduate Research Training Project of Liaoning Normal University (No. CX202102008, 202110165098).

CRediT authorship contribution statement **Ailu Cui:** Data curation, Writing- Original draft preparation, **Zuan Yang:** Data curation, Writing- Original draft preparation, **Xuewei Feng:** Data curation, Writing- Original draft preparation, **Huanying Zhao:** Formal analysis, Writing- Reviewing and Editing, **Peiran Meng:** Formal analysis, Writing- Reviewing and Editing, **Yanxuan Xie:** Formal analysis, Writing- Reviewing and Editing, **Linan Miao:** Formal

analysis, Writing- Reviewing and Editing, **Yue Sun:** Conceptualization, Methodology.

Declarations

Competing interest The authors declare that they have no known competing financial interests or personal relationships that could have appeared to influence the work reported in this paper.

References

1. Che Lah NF, Ahmad AL, Mohd Amri MH, Chin JY (2022) Configuration of molecularly imprinted polymers for specific uptake of pharmaceutical in aqueous media through radical polymerization method. J Polym Res 29
2. Paruli E III, Soppera O, Haupt K, Gonzato C (2021) Photopolymerization and photostructuring of molecularly imprinted polymers. ACS Appl Polym Mater 3:4769–4790
3. Ozcelikay G, Kaya SI, Ozkan E, Cetinkaya A, Nemutlu E, Kır S, Ozkan SA (2022) Sensor-based MIP technologies for targeted metabolomics analysis. TrAC Trends Anal Chem 146
4. Yang Z, Yang K, Cui Y, Shah T, Ahmad M, Zhang Q, Zhang B (2021) Synthesis of surface imprinted polymers based on wrinkled flower-like magnetic graphene microspheres with favorable recognition ability for BSA. J Mater Sci Technol 74:203–215
5. Ferreira JB, de Jesus MC, Dinali LAF, Filho JFA, Silva CF, Borges KB, Romao W (2021) Molecularly imprinted polymers as a selective sorbent for forensic applications in biological samples-a review. Anal Bioanal Chem 413:6013–6036
6. He S, Zhang L, Bai S, Yang H, Cui Z, Zhang X, Li Y (2021) Advances of molecularly imprinted polymers (MIP) and the application in drug delivery. Eur Polym J 143
7. Motia S, Bouchikhi B, El Bari N (2021) An electrochemical sensor based on molecularly imprinted polymer conjointly with a voltammetric electronic tongue for quantitative diphenyl phosphate detection in urine samples from cosmetic product users. Sens Actuators B Chem 332
8. Zaidi SA (2021) An overview of bio-inspired intelligent imprinted polymers for virus determination. Biosensors (Basel) 11
9. Ali GK, Omer KM (2022) Molecular imprinted polymer combined with aptamer (MIP-aptamer) as a hybrid dual recognition element for bio(chemical) sensing applications. Review Talanta 236:122878
10. Hu W, Xu L (2021) Investigation of eATRP for a carboxylic-acid-functionalized ionic liquid monomer. Macromol Chem Phys 222
11. Isse AA, Lorandi F, Gennaro A (2019) Electrochemical approaches for better understanding of atom transfer radical polymerization. Curr Opin Electrochem 15:50–57
12. Yang W, Fang Q, Zhang L, Yin H, Wu C, Zhang W, Huang W, Ni X (2021) Synthesis and characterization of an innovative molecular imprinted polymers based on CdTe QDs fluorescence sensing for selective detection of sulfadimidine. J Polym Res 28
13. Hu Y, Liang B, Fang L, Ma G, Yang G, Zhu Q, Chen S, Ye X (2016) antifouling zwitterionic coating via electrochemically mediated atom transfer radical polymerization on enzyme-based glucose sensors for long-time stability in 37 degrees C serum. Langmuir 32:11763–11770
14. Bortolamei N, Isse AA, Magenau AJ, Gennaro A, Matyjaszewski K (2011) Controlled aqueous atom transfer radical polymerization with electrochemical generation of the active catalyst. Angew Chem Int Ed Engl 50:11391–11394
15. Michieletto A, Lorandi F, De Bon F, Isse AA, Gennaro A (2019) Biocompatible polymers via aqueous electrochemically mediated atom transfer radical polymerization. J Polym Sci 58:114–123
16. Fantin M, Lorandi F, Isse AA, Gennaro A (2016) Sustainable electrochemically-mediated atom transfer radical polymerization with inexpensive non-platinum electrodes. Macromol Rapid Commun 37:1318–1322
17. Sun Y, Lathwal S, Wang Y, Fu L, Olszewski M, Fantin M, Enciso AE, Szczepaniak G, Das S, Matyjaszewski K (2019) Preparation of well-defined polymers and DNA–polymer bioconjugates via small-volume eATRP in the presence of air. ACS Macro Lett 8:603–609
18. Sajid M, Plotka-Wasylka J (2022) Green analytical chemistry metrics: A review. Talanta 238:123046
19. Sripirom J, Sim WC, Khunkaewla P, Suginta W, Schulte A (2018) simple and economical analytical voltammetry in 15 mul volumes: Paracetamol voltammetry in blood serum as a working example. Anal Chem 90:10105–10110
20. Chmielarz P, Yan J, Krys P, Wang Y, Wang Z, Bockstaller MR, Matyjaszewski K (2017) Synthesis of nanoparticle copolymer brushes via surface-initiated seATRP. Macromolecules 50:4151–4159
21. Xu X, Xu X, Zeng Y, Zhang F (2021) Oxygen-tolerant photoinduced metal-free atom transfer radical polymerization. J Photochem Photobiol A Chem 411
22. Llorente O, Agirre A, Calvo I, Olaso M, Tomovska R, Sardon H (2021) Exploring the advantages of oxygen-tolerant thiol-ene polymerization over conventional acrylate free radical photopolymerization processes for pressure-sensitive adhesives. Polym J 53:1195–1204
23. Poulose S, Jönkkäri I, Hedenqvist MS, Kuusipalo J (2021) Bioplastic films with unusually good oxygen barrier properties based on potato fruit-juice. RSC Adv 11:12543–12548
24. Enciso AE, Fu L, Russell AJ, Matyjaszewski K (2018) A breathing atom-transfer radical polymerization: fully oxygen-tolerant polymerization inspired by aerobic respiration of cells. Angew Chem Int Ed Engl 57:933–936
25. Liarou E, Whitfield R, Anastasaki A, Engelis NG, Jones GR, Velonia K, Haddleton DM (2018) Copper-mediated polymerization without external deoxygenation or oxygen scavengers. Angew Chem Int Ed Engl 57:8998–9002
26. Wang H, Li F, Dong Y, Li Z, Wang G-L (2019) Ferricyanide stimulated cathodic photoelectrochemistry of flower-like bismuth oxyiodide under ambient air: A general strategy for robust bioanalysis. Sens Actuators, B Chem 288:683–690
27. Kim SY, Park CS, Hosseini S, Lampert J, Kim YJ, Nazar LF (2021) Inhibiting oxygen release from Li-rich, Mn-rich layered oxides at the surface with a solution processable oxygen scavenger polymer. Adv Energy Mater 11
28. Ma P, Ma X, Chen F (2021) The construction of stimulus-responsive film electrode by the Cu-catalyzed radical polymerization and its application in multi-valued biologic systems. Electroanalysis 33:2437–2444
29. Wang J, Tian M, Li S, Wang R, Du F, Xue Z (2018) Ligand-free iron-based electrochemically mediated atom transfer radical polymerization of methyl methacrylate. Polym Chem 9:4386–4394
30. Park S, Chmielarz P, Gennaro A, Matyjaszewski K (2015) Simplified electrochemically mediated atom transfer radical polymerization using a sacrificial anode. Angew Chem Int Ed Engl 54:2388–2392
31. Zaborniak I, Chmielarz P (2020) Miniemulsion switchable electrolysis under constant current conditions. Polym Adv Technol 31:2806–2815
32. Chmielarz P, Sobkowiak A (2017) Ultralow ppm seATRP synthesis of PEO-b-PBA copolymers. J Polym Res 24
33. Zaborniak I, Chmielarz P, Martinez MR, Wolski K, Wang Z, Matyjaszewski K (2020) Synthesis of high molecular weight poly(n-butyl acrylate) macromolecules via seATRP: From polymer stars to molecular bottlebrushes. Eur Polym J 126

34. Chmielarz P, Park S, Sobkowiak A, Matyjaszewski K (2016) Synthesis of β-cyclodextrin-based star polymers via a simplified electrochemically mediated ATRP. Polymer 88:36–42
35. Szczepaniak G, Fu L, Jafari H, Kapil K, Matyjaszewski K (2021) Making ATRP more practical: oxygen tolerance. Acc Chem Res 54:1779–1790
36. Liu H, Yu H (2019) Ionic liquids for electrochemical energy storage devices applications. J Mater Sci Technol 35:674–686
37. Shahriman MS, Mohamad S, Mohamad Zain NN, Alias Y, Chandrasekaram K, Raoov M (2021) Paper-based polymeric ionic liquid for thin film micro extraction of sulfonamides in environmental water samples prior to HPLC-DAD analysis. Microchem J 171
38. Xie W, Zhang J, Zeng Y, Wang H, Yang Y, Zhai Y, Miao D, Li L (2020) Highly sensitive and selective detection of 4-nitroaniline in water by a novel fluorescent sensor based on molecularly imprinted poly(ionic liquid). Anal Bioanal Chem 412:5653–5661
39. Lu Y, Hu J, Zeng Y, Zhu Y, Wang H, Lei X, Huang S, Guo L, Li L (2020) Electrochemical determination of rutin based on molecularly imprinted poly (ionic liquid) with ionic liquid-graphene as a sensitive element. Sens Actuators B Chem 311
40. Wu Y, Wang Y, Wang X, Wang C, Li C, Wang Z (2019) Electrochemical sensing of α-fetoprotein based on molecularly imprinted polymerized ionic liquid film on a gold nanoparticle modified electrode surface. Sensors (Basel) 19
41. Sun Y, Zhang J, Li J, Zhao M, Liu Y (2017) Preparation of protein imprinted polymers via protein-catalyzed eATRP on 3D gold nanodendrites and their application in biosensors. RSC Adv 7:28461–28468
42. Sun Y, Du H, Deng Y, Lan Y, Feng C (2015) Preparation of polyacrylamide via surface-initiated electrochemical-mediated atom transfer radical polymerization (SI-eATRP) for Pb^{2+} sensing. J Solid State Electrochem 20:105–113
43. Sun Y, Feng X, Hu J, Bo S, Zhang J, Wang W, Li S, Yang Y (2020) Preparation of hemoglobin (Hb)-imprinted poly(ionic liquid)s via Hb-catalyzed eATRP on gold nanodendrites. Anal Bioanal Chem 412:983–991
44. Jijana AN, Mphuthi N, Shumbula P, Vilakazi S, Sikhwivhilu L (2021) The ultra-sensitive electrochemical detection of As(III) in ground water using disposable L-cysteine/Lipoic Acid functionalised gold nanoparticle modified screen-printed electrodes. Electrocatalysis 12:310–325
45. Paixão TRLC (2020) Measuring electrochemical surface area of nanomaterials versus the Randles−Ševčík equation. ChemElectroChem 7:3414–3415
46. Yang Y, Sun Y, Jin M, Bai R, Liu Y, Wu Y, Wang W, Feng X, Li S (2020) Fabrication of Superoxide Dismutase (SOD) imprinted poly(ionic liquid)s via eATRP and its application in electrochemical sensor. Electroanalysis 32:1772–1779
47. Yan CN, Liu Q, Xu L, Bai LP, Wang LP, Li G (2019) Photoinduced metal-free surface initiated ATRP from hollow spheres surface. Polymers (Basel) 11
48. Bagus PS, Nelin CJ, Brundle CR, Crist BV, Lahiri N, Rosso KM (2021) Combined multiplet theory and experiment for the Fe 2p and 3p XPS of FeO and Fe_2O_3. J Chem Phys 154:094709
49. Wei Y, Zeng Q, Huang J, Guo X, Wang L, Wang L (2020) Preparation of gas-responsive imprinting hydrogel and their gas-driven switchable affinity for target protein recognition. ACS Appl Mater Interfaces 12:24363–24369
50. Bai R, Sun Y, Zhao M, Han Z, Zhang J, Sun Y, Dong W, Li S (2021) Preparation of IgG imprinted polymers by metal-free visible-light-induced ATRP and its application in biosensor. Talanta 226:122160
51. Sun Y, Du H, Lan Y, Wang W, Liang Y, Feng C, Yang M (2016) Preparation of hemoglobin (Hb) imprinted polymer by Hb catalyzed eATRP and its application in biosensor. Biosens Bioelectron 77:894–900
52. Bo S, Sun Y, Li S, Zhou Y, Feng X, Li C (2021) Preparation of hemoglobin (Hb) imprinted polymers with CO_2 response and its biosensing application. J Solid State Electrochem 25:1645–1655
53. Motia S, Bouchikhi B, El Bari N (2021) An electrochemical molecularly imprinted sensor based on chitosan capped with gold nanoparticles and its application for highly sensitive butylated hydroxyanisole analysis in foodstuff products. Talanta 223:121689
54. Kalaiyarasan G, Joseph J (2019) Cholesterol derived carbon quantum dots as fluorescence probe for the specific detection of hemoglobin in diluted human blood samples. Mater Sci Eng C Mater Biol Appl 94:580–586
55. Liu Y, Wang Y, Jiang K, Sun S, Qian S, Wu Q, Lin H (2020) A persistent luminescence-based label-free probe for the ultrasensitive detection of hemoglobin in human serum. Talanta 206:120206
56. Duan H, Wang X, Wang Y, Li J, Luo C (2015) Bioreceptor multiwalled carbon nanotubes@Fe_3O_4@SiO_2–surface molecular imprinted polymer in an ultrasensitive chemiluminescent biosensor for bovine hemoglobin. RSC Adv 5:88492–88499
57. Li N, Liu X, Zhu J, Zhou B, Jing J, Wang A, Xu R, Wen Z, Shi X, Guo S (2020) Simple and sensitive detection of acrylamide based on hemoglobin immobilization in carbon ionic liquid paste electrode. Food Control 109
58. Wang Z, Li F, Xia J, Xia L, Zhang F, Bi S, Shi G, Xia Y, Liu J, Li Y, Xia L (2014) An ionic liquid-modified graphene based molecular imprinting electrochemical sensor for sensitive detection of bovine hemoglobin. Biosens Bioelectron 61:391–396